

## Effects of Oxygen Partial Pressure During Sintering of FR MOX Fuels at Laboratory and Industrial Scales

Stéphane Vaudez\*, J. Martinez, F. Lebreton, C. Chambon, G. Court, C. Rieseemann-Gazeau

*CEA, DEN, DMRC, SFMA, CEA Marcoule, F-30207 Bagnols sur Cèze, France*

*\* Corresponding author at CEA, DEN, DMRC, SFMA, CEA Marcoule, F-30207 Bagnols sur Cèze, France.*

*Phone: +334 42 25 31 90, Fax: +334 42 25 47 17, E-mail: stephane.vaudez@cea.fr*

### Abstract

France intends to build a sodium-cooled fast reactor (SFR) prototype called ASTRID - for Advanced Sodium Technological Reactor for Industrial Demonstration - in preparation of the industrial deployment of such sodium fast reactors in the future. Its mixed oxide (MOX) fuels will be produced by a new industrial-scale core fabrication facility named AFC<sup>1</sup>, which is still under development.

The fabrication process of MOX fuel is based on powder metallurgy processes. The UO<sub>2</sub> and PuO<sub>2</sub> mixture is pelletized and then sintered at about 1700°C under reducing atmosphere of Ar/4%H<sub>2</sub>/H<sub>2</sub>O. Fuel has to be in compliance with specifications. In particular, the O/M (atomic oxygen to metal ratio) has to be hypostoichiometric and close to 1.97 and the microstructure has to be dense, around 95 %Th.D. The O/M and microstructure can affect numerous properties of the fuel during operation including thermal conductivity, mechanical properties and fuel-cladding interactions. To meet these requirements, better knowledge of sintering at laboratory and industrial scale is needed.

An original analysis method has been therefore developed for a better understanding of the O/M ratio evolution and densification mechanisms during the sintering step. By coupling a dilatometer with an oxygen zirconia probe, it is possible to identify the different redox phenomena and to plot the evolution of the O/M of the oxides versus time during the densification process. This innovative method is helpful to understand how gas and fuel interact. Whereas it was difficult to predict a precise final O/M, this new method produces the expected ratio every time.

This paper highlights the different final O/M values and microstructure, particularly in terms of microcracking, obtained during sintering in a continuous industrial or laboratory furnace. The impact of the evolution of moisture content in the gas is explained. Based on these results, a multiphysic model is being built to obtain a better knowledge of the interaction with MOX fuel and the surrounding atmosphere. Then, some recommendations can be made about the sintering atmosphere to improve industrial cycles and optimize fuel characteristics in order to obtain an O/M as close as possible to the target value and the right microstructure.

### Keywords

Nuclear fuels; mixed oxide of uranium and plutonium; oxygen stoichiometry; oxygen partial pressure; sintering; cracks

---

<sup>1</sup> French abbreviation for *Atelier de Fabrication des Coeurs*

## 1. Introduction

France intends to build a sodium-cooled fast reactor (SFR) prototype called ASTRID - for Advanced Sodium Technological Reactor for Industrial Demonstration - in preparation of the industrial deployment of such sodium fast reactors in the future [1, 2]. Its mixed oxide (MOX) fuels will be produced by a new industrial-scale core fabrication facility named AFC, which is still being designed.

The fabrication process of mixed uranium plutonium oxide (MOX) for Sodium Fast Reactor (SFR) is based on powder metallurgy processes including  $\text{UO}_2$  and  $\text{PuO}_2$  powder mixing step to reach the final Pu concentration in the range between 23 to 35%wt. The mixture is pelletized and then sintered at about  $1700^\circ\text{C}$  under reducing atmosphere of  $\text{Ar}/4\%\text{H}_2/\text{H}_2\text{O}$ . To control the fuel characteristics (e.g. density and O/M ratio), it is crucial to control the sintering atmosphere and especially the oxygen partial pressure ( $p\text{O}_2$ ) throughout the thermal cycle [1, 2]. It's the reason why an original analysis method has been developed for a better understanding of the densification mechanisms and the O/M ratio evolution during the sintering step. This paper is focused on the description of this technics, its application to the  $\text{UO}_2$ ,  $\text{PuO}_2$  and  $\text{UPuO}_2$  sintering and the transposition in industrial furnace.

## 2. Experimental

### 2.1 Raw materials and sample preparation

Scanning electron microscopy (SEM) images (figure 1) show that  $\text{UO}_2$  powder is composed of  $50\ \mu\text{m}$  large spherical agglomerates consisting of crystallites of submicrometer size.  $\text{PuO}_2$  powder consists in  $0.5\ \mu\text{m}$  thick flakes. Specific surface areas measured by the BET method, O/M analysis as well as other characteristics of the raw powders are summarized in Table 1.

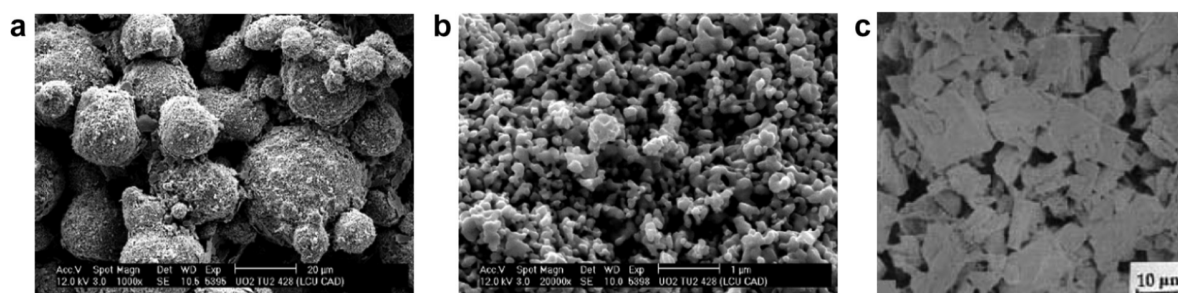


Figure 1 : SEM micrographs of  $\text{UO}_2$  precursor powder (a) agglomerates, (b) crystallites and (c)  $\text{PuO}_2$  precursor powder.

Table 1: characteristics of the starting powders and green pellets.

Characteristics	Unit	$\text{UO}_2$	$\text{PuO}_2$
Specific surface area ( $\pm 0.5$ )	$\text{m}^2.\text{g}^{-1}$	3.3	3.9
Oxygen to metal ratio		2.11	2.00
Theoretical density TD	$\text{g}.\text{cm}^{-3}$	10.96	11.46
Green density ( $\pm 0.2$ )	$\text{g}.\text{cm}^{-3}$	5.7	6.6

The  $\text{UO}_2/\text{PuO}_2$  mixture was prepared at the LEFCA facility (CEA Cadarache, France) by a powder metallurgy process optimized for small amounts of powder (40 g). 70% of  $\text{UO}_{2+x}$  and 30% of  $\text{PuO}_2$  powders were mixed for 4 h in a ball mill using metallic uranium balls. Then, the mixture was sieved through a  $160\ \mu\text{m}$  screen. This powder preparation results in an intimate contact between both precursors without affecting the specific surface area. 1 gram of each powder, i.e.  $\text{UO}_2$ ,  $\text{PuO}_2$  and 70%

UO<sub>2</sub> + 30% PuO<sub>2</sub> mixture, were pressed into green cylinders of 6 mm in diameter and height. An uniaxial press was used for making green pellets.

## 2.2 Dilatometry experiments

The densification behavior of the pellet and the  $pO_2$  evolution of the sintering gas were assessed using a vertical dilatometer (SETARAM TMA92-16.18) coupled with a SETNAG<sup>®</sup> zirconia probe. The latter is implemented at the furnace outlet (figure 2) and operates at 650°C with a metallic reference. The zirconia probe measures continuously the amount of O<sub>2</sub> exchanged between the solid sample and its atmosphere. The incoming H<sub>2</sub> partial pressure is measured with gas chromatography (typically 4 vol.%) and the humidity rate of the inlet gas is determined with a capacity probe device (from Vaisala company). A blank measurement of  $pO_2$  was taken prior to any experiment in order to assess the  $pO_2$  of the carrier gas. The thermal cycle consists in heating sample at 60°C/h up to 1600°C during 4h and cooling down with a rate of 420°C/h. The gas flow rate is 8 L.H-1 which corresponds to around 150 litres of gas per gram of MOX fuel during the thermal cycle.

The  $pO_2$  monitored throughout the sintering cycle with the sample combines the oxygen of the carrier gas and the oxygen added (or deducted) from the redox reactions during the sintering so that these measurements can be used to evaluate the redox reactions of actinide oxides throughout the sintering thermal cycle [3], as illustrated in the next section.

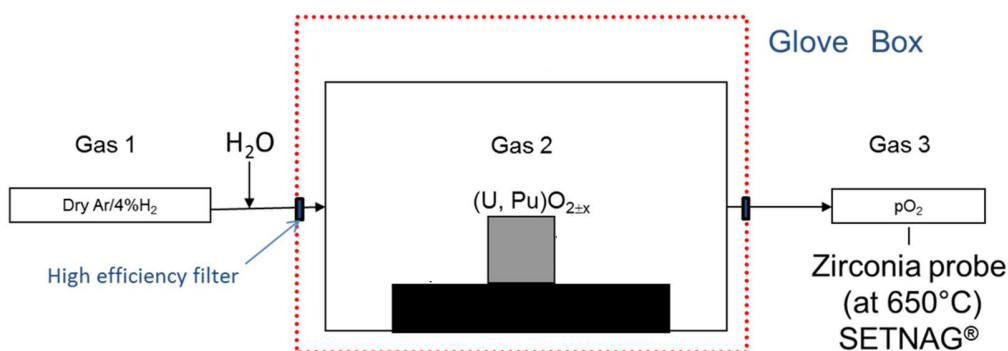


Figure 2: Schematic view of the furnace device coupled with the zirconia probe to control the  $pO_2$  evolution of the sintering gas throughout the thermal cycle.

## 3. Results and Discussion

### 3.1 Densification and Solid/Gas equilibrium during sintering

The experiments realized on UO<sub>2</sub> and PuO<sub>2</sub> samples are illustrated in figure 3a and 3b. The relative shrinkage  $\Delta L/L_0$  (dotted lines) is given versus temperature as well as the measured  $pO_2$  (red lines) during heating (right arrow) and cooling (left arrow). Grey curves are the  $pO_2$  measurement results without any sample: it can be checked that there is no change during the whole thermal cycle.

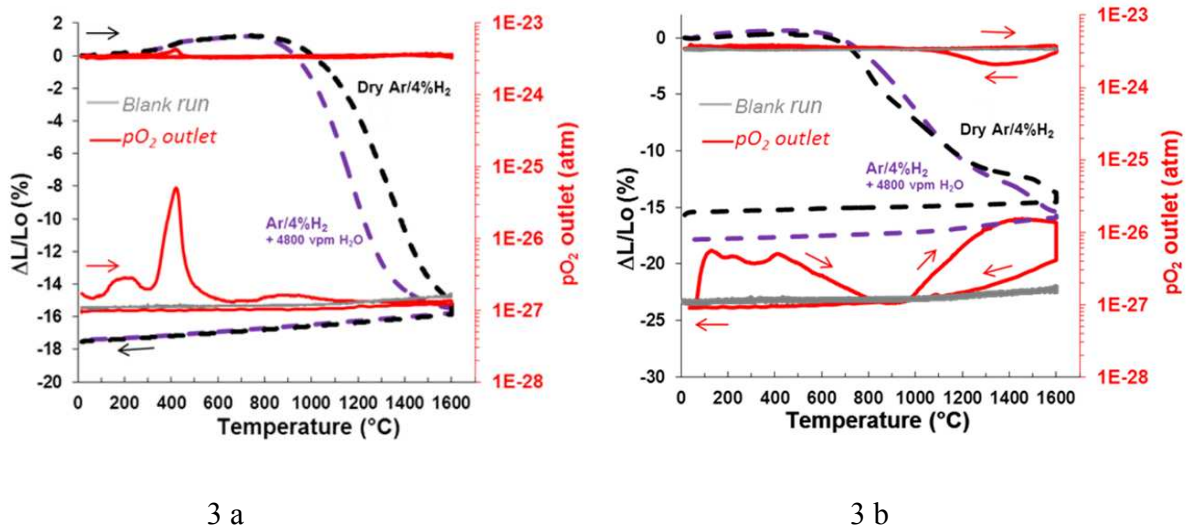


Figure 3: dilatometric studies of the shrinkage of  $UO_2$  samples a) and  $PuO_2$  samples b) under dry  $Ar/4\%H_2$  (black curve) and  $Ar/4\%H_2 + 4800 \text{ vpm } H_2O$  (violet curve) combined with  $pO_2$  gas outlet measurement (red curve with wet atmosphere on the top, dry atmosphere at the bottom).

Under wet  $Ar/4\%H_2$ , the shrinkage temperature of  $UO_2$  is shifted to the lower temperatures compared to the experiment under dry  $Ar/4\%H_2$ , consistent with the literature [2]. A large  $O_2$  release peak between 300 and 600°C is directly linked to the reduction of  $UO_{2+x}$  into  $UO_{2.00}$ , occurring before the densification (note that the peak at lower temperature is due to the water desorption from the fuel surface) [2]. Above 600°C and during cooling, the sample is close to the thermodynamic equilibrium with the carrier gas and the slight  $pO_2$  variations correspond to the slight O/U ratio evolution around 2.00.

As regards  $PuO_2$  sample, the shrinkage curve under wet  $Ar/4\%H_2$  is slightly delayed in temperature up to 1200°C compared to that in dry  $Ar/4\%H_2$ , in contrast to the previous case. Above 1200°C, the reverse occurs. Two large peaks of  $O_2$  release are recorded. The first peak up to 800°C is related to the elimination of adsorbed species, as observed elsewhere [4]. The second peak within the temperature range of 1000-1600°C and during the plateau is consistent with the reduction of  $PuO_2$  into  $PuO_{2-x}$ . During cooling,  $pO_2$  decreases in each case, but the  $pO_2$  curve is above the blank curve in dry atmosphere and below in wet one, pointing out in the latter case an oxidation reaction.

### 3.2 O/M evolution

Knowing the  $pO_2$  evolution at each time of the sintering cycle, the O/M evolution is calculated according to the temperature [5] as illustrated for  $UO_2$ ,  $PuO_2$  and a mixture of  $UO_2$  and  $PuO_2$  (30wt%) in figure 4.

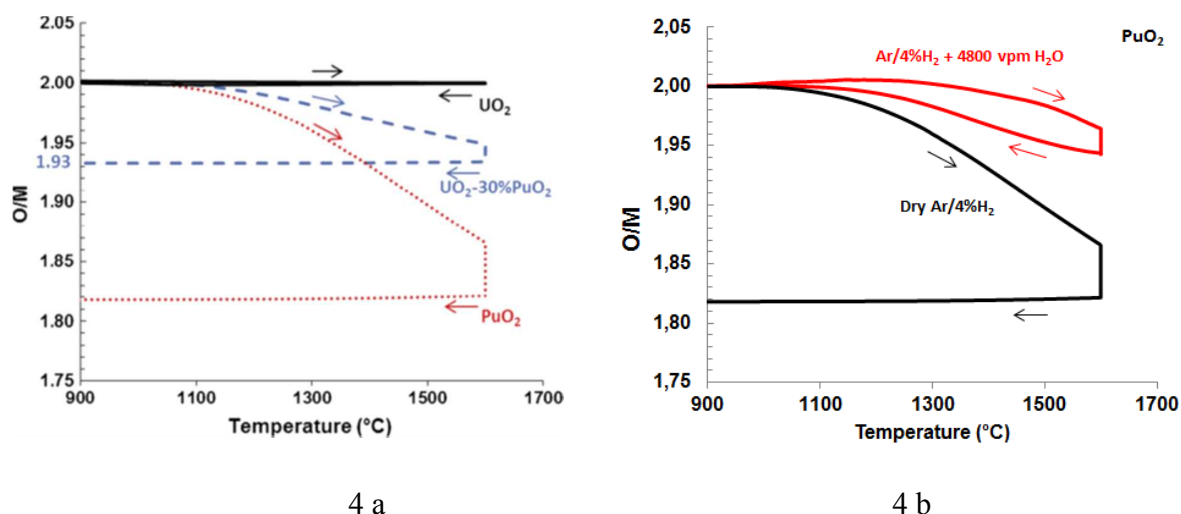


Figure 4 : experimental variation of the O/M ratio during the sintering of  $\text{PuO}_2$ ,  $\text{UO}_2$  and  $\text{UO}_2\text{-30\%Pu}$  under  $\text{Ar}/4\%\text{H}_2 + 50 \text{ vpm H}_2\text{O}$  [3] and  $\text{PuO}_2$  under  $\text{Ar}/4\%\text{H}_2 + 4800 \text{ vpm H}_2\text{O}$  [5] (red curve).

It can be noted that there is no evolution of O/U above  $1000^\circ\text{C}$  for  $\text{UO}_2$ , as expected from a thermodynamic point of view (figure 4a).

Under dry and wet sintering gas, a continuous decrease in the O/M can be observed for  $\text{PuO}_2$  during heating and the plateau (Figure 4b), as expected according to the thermodynamic calculations [6]. The lower the  $p\text{O}_2$ , the smaller the O/M at high temperature. The difference between wet and dry atmosphere is however significant during the cooling. Under wet atmosphere, the sample gets oxidized again and the O/M ratio tends to 2.00 around  $1000^\circ\text{C}$ , as expected. On the contrary, no O/M evolution was seen during cooling under dry atmosphere. More generally, such a significant deviation between thermodynamic and experimental O/M is observed for MOX pellets with high Pu content whatever the temperature in reducing conditions ( $\text{O/M} < 2.00$ ) [3, 5] as observed in figure 4a.

### 3.3 Discussion and first result on transposition at an industrial scale

In the past, FR MOX pellets were fabricated at industrial scale in the ATPu<sup>2</sup> (Atelier de Technologie du Plutonium), where Phenix and Superphenix fuels were produced between 1974 and 1999. Pellets fabricated in the ATPu exhibited microstructure free of cracks and a final O/M between 1.96 and 1.98, even though the furnace was operated with a "dry"<sup>3</sup>  $\text{Ar}/4\%\text{H}_2$  gas.

In the laboratory furnace, when "dry"  $\text{Ar}/4\%\text{H}_2$  gas is used during sintering, the final O/M is less than 1.94. To reach the value of 1.97, around 200 vpm of moisture must be added to the gas.

<sup>2</sup> French abbreviation for "technological facility for plutonium"

<sup>3</sup> The sintering gas is never completely dry. It is generally agreed that it contains at least 50 vpm of moisture in the lab furnace. The moisture rate in the sintering gas of the ATPu furnace is not known.

Unfortunately, microcracks appears in the pellet rim, which were never observed in the industrial production (figure 5).

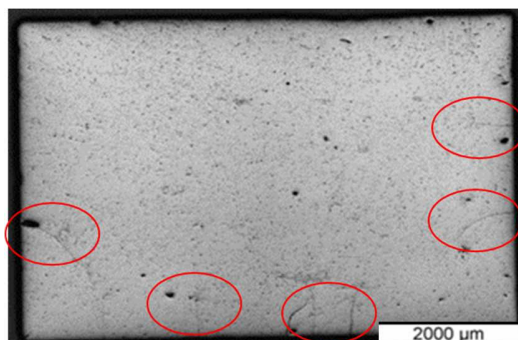


Figure 5: Microstructure with rim microcracks for an O/M of 1.97 obtained with a constant humidity rate of 200 ppm  $H_2O$  during the sintering.

Such differences can be explained by the very different sintering furnace technologies:

- in the laboratory batch furnaces, the sintering gas comes in contact with the pellets and is then directly evacuated, as illustrated Figure 6a,
- in the industrial continuous furnace, the sintering gas flows in the opposite direction of the pellet conveyer. Thus, the sintering gas meets firstly the sintered pellets before licking the pre-sintered and green ones as presented figure 6b. Due to the plutonium reduction, the sintering gas is therefore much more enriched with moisture at the furnace inlet than at the outlet.

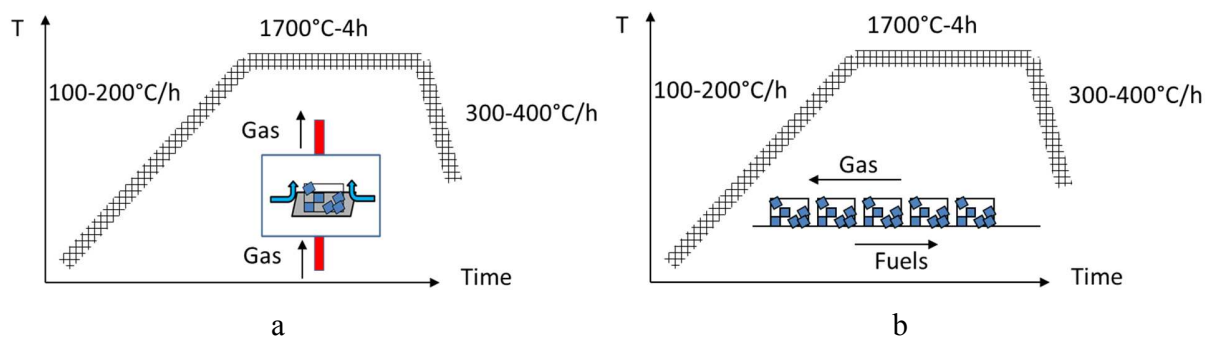


Figure 6 : Schemes of the sintering cycles at the laboratory a) and at the industrial scales b) of SFR MOX fuels.

Transposing the results obtained with a batch furnace into a continuous and countercurrent furnace or vice-versa is not trivial and requires a modeling work involving data from different nature (aerualics, thermodynamics, transport, kinetics, etc.). These data are presently missing. Nevertheless, a rough assessment of the  $H_2O$  content evolution of the sintering gas in a continuous furnace is calculated and illustrated figure 7. It takes into account data coming from device described § 2.2 and results coming from the  $UO_2/30\%Pu$  experiment [3] presented figure 4. Therefore, it is considered for the continuous furnace a train of 30%Pu MOX pellets with a gas flow rate of 150 L/g of gas, a residence

time in the furnace of 19h and an initial moisture rate of 50 vpm in Ar/4%H<sub>2</sub>. At this stage, no fuel/sintering gas reactions are considered.

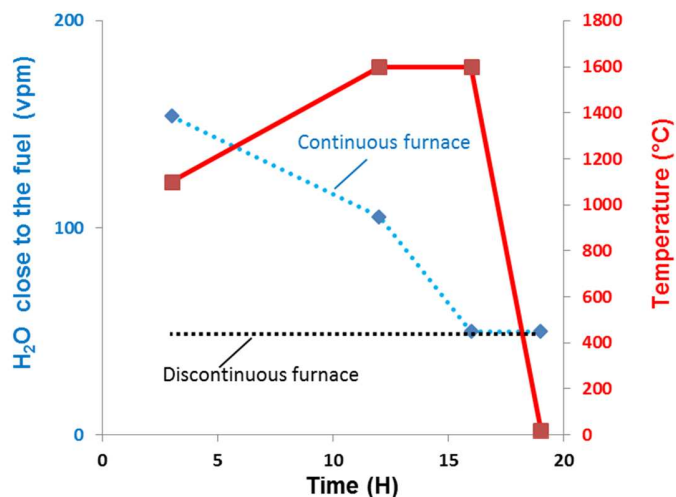


Figure 7: H<sub>2</sub>O evolution in Ar/4%H<sub>2</sub> in the case of a discontinuous furnace and a continuous furnace with gas flow in the opposite direction of the pellets.

In the case of a continuous furnace, the H<sub>2</sub>O enrichment of the gas is significant when the green pellets enter the furnace and decreases continuously during the sintering cycle to be completely dry when the pellets leave the furnace. At 1100°C, for example, the gas contains 150 vpm of H<sub>2</sub>O while the inlet gas contains 50 vpm H<sub>2</sub>O. This enrichment is obviously proportional to the number/weight of pellets in the furnace and to the gas flow.

To simulate the continuous sintering furnace cycles in a batch furnace, it is therefore necessary to adjust continuously the moisture content of the inlet gas. This moisture evolution during sintering can explain the O/M and microstructure difference previously mentioned between MOX pellets sintering in “dry” atmosphere in the ATPu (industrial furnace) and in the LEFCA Facility (batch furnace).

With this result, the sintering cycle in the batch furnace has been successfully optimized: it consists in heating MOX sample under Ar/4%H<sub>2</sub> at relatively high moisture content (close to 500 vpm) up to the plateau at 1700°C, then to reduce linearly the moisture rate during the cooling until almost dry at about 1000°C.

In such conditions, the fuel microstructure is free of rim microcracks (figure 8) and the final O/M is equal to 1.97. The microcrack disappearance may be explained by a low O/M variation of the fuel during the shrinkage, contrary to what was measured in the previous sintering conditions (figure 4).

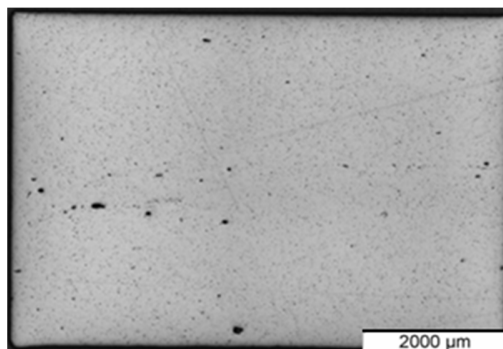


Figure 8: Microstructure free of microcracks for an O/M of 1.97 obtained with a sintering with a humidity change during sintering cycle.

That suggests that the rim micro-cracking of the sintered pellets may be related to oxygen gradient between the periphery and the heart of the fuel, since it has been shown that the equilibrium state is never reached in a “dry” sintering gas. The H<sub>2</sub>O cycle optimization will largely contribute to control both the global and the gradient of O/M and consequently the microstructure.

### 3.4 Numerical modelling

It was shown that the technological difference between a continuous and discontinuous furnace induces different characteristics of the surrounding atmosphere, even if the outlet gas is similar. To improve the knowledge of the atmosphere effects on the MOX sintering, a multiphysics model is being built to forecast the MOX characteristics and more specifically, the global and local O/M as well as the stress field during the sintering stage. This model is developed at a macroscale level. The system of interest is reduced to the MOX fuel sample and the surrounding atmosphere. The MOX fuel is represented by a porous system with a solid MOX phase and an atmosphere phase in the porosity and outside the pellet.

The physical description of the system requires models from thermal science, fluid mechanics and chemistry to take into account the evolution of oxygen partial pressure or water vapor in the atmosphere. These three models are linked to each other, as schematized in figure 9. The heat transfer influences the fluid mechanics due to the variation of fluid properties with the temperature. And reversely, the fluid velocity influences the temperature field because of the convection flow. The chemical reaction is influenced by the temperature field through the reaction kinetic. The conservation of the chemical species is influenced by the fluid flow and by the convection flow too. To simplify the system, the chemical reaction is supposed to be athermic. So the chemical reaction does not influence the heat transfer equation. The variation of gas density is supposed to be constant and the chemical reaction does not influence the fluid mechanics.

For the solid MOX fuel part, the experimental data show that the physics of interest are thermal and electrochemical science to predict the O/M variations and solid mechanics. In the figure 9, the solid mechanics are divided into two parts: sintering part and mechanics part. This distinction is made to have a better phenomenological representation.

The thermal effects influence:

- the electrochemical reaction by the reaction kinetic,
- the mechanics part by the thermal strain,
- the sintering part by the evolution of density.



The electrochemical science interacts with the solid mechanic through the strain induced by the variation of the MOX fuel stoichiometry [7, 8]. This strain is called “chemical strain”. The evolution of MOX stoichiometry influences the sintering part through the variation of bulk and grain boundary diffusion coefficient. Reversely, the variation of density influences the specific surface area in the electrochemical reaction. Firstly, the solid mechanic interacts with the heat transfer equation by the variation of the thermal properties due to the variation of the density. Finally, the viscoplasticity phenomenon is assumed not to generate heat source.

The boundary conditions of these different physics are:

- the fluid rate and surrounding total pressure for the fluid mechanics,
- the inlet gas composition for the atmosphere chemical reaction,
- the heat element of furnace for the thermal part and the support contact for the solid mechanic.

For the electrochemical part, the boundary condition is the surface exchange reaction.

Finally, this multiphysic model is implemented in the finite elements software: Comsol Multiphysics. To build this complex model, it is divided in several step:

- first, the atmosphere is simulated without MOX sample, so that the atmosphere differences between the two furnaces are highlighted ;
- the second step is focused on the chemical MOX behavior (O/M modeling) with the applied atmosphere condition (temperature, oxygen partial pressure ... ) ;
- The third step is focused on the sintering part ;
- Finally all the previous steps are coupled together.

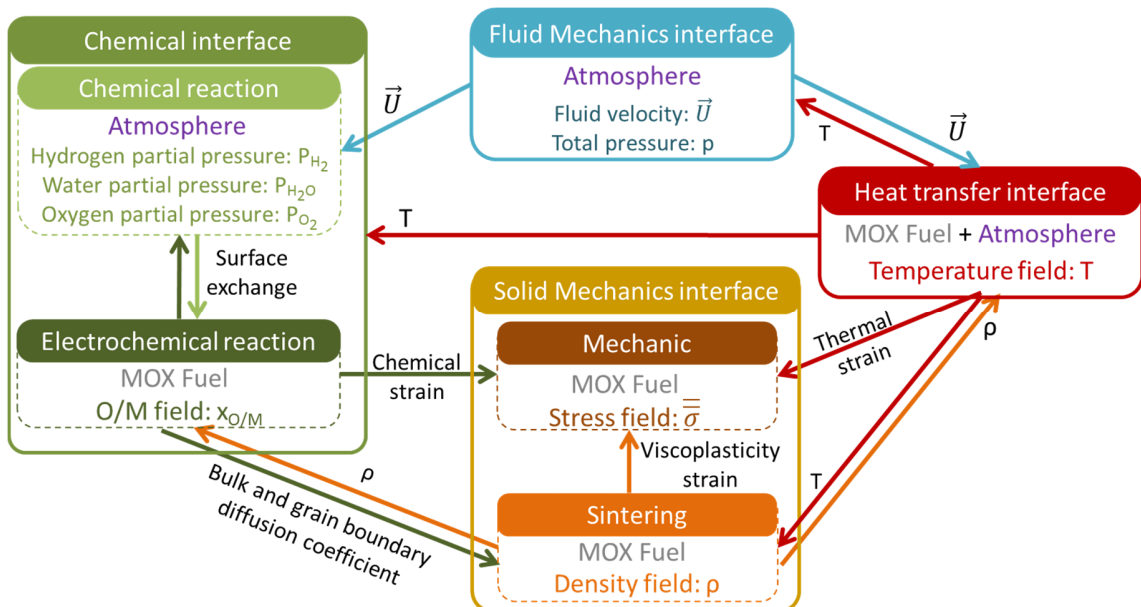


Figure 9: Schema of the multiphysic model.

#### 4. Conclusions and outlook

By coupling a dilatometer and a zirconia probe, it is possible to identify the different redox phenomena and to assess the evolution of the O/M ratio of the oxides at each time of the densification process. It is shown that under certain conditions, the thermodynamic equilibrium between gas and fuel is long to be reached so that it can be difficult to control and predict O/M ratio, especially for SFR-type fuel (sintered in reductive conditions).

At laboratory scale, sintering conditions have had to be improved in order to obtain pellets with the requested O/M and free of rim microcracks. These conditions consist in adjusting the moisture rate of the sintering gas all along the thermal cycle. The sintering conditions optimized in this paper are not necessarily reproducible for other furnace technology since they depend on furnace aerualics, fuel quantity to be sintered, fuel geometry, humidity rate, etc...

To improve the knowledge of the atmosphere effects on the MOX characteristics and to predict these latter, a multiphysic model is being built. Thanks to experimental data and to the numerical modelling approach, it should be possible to recommend the best sintering atmosphere and thermal cycle to meet the fuel specifications while minimizing the experimental work.

#### 5. References

- [1] Hj. Matzke, J. Chem. Soc. Faraday Trans. 83 (1987) 1121.
- [2] S. Berzati, S. Vaudez, R. C. Belin, J. Lechelle, Y. Marc, JC. Richaud, JM. Heintz J. Nuc. Mat., 447 (2014) 115-124.
- [3] S. Vaudez, J. Lechelle, S. Berzati, JM. Heintz J. Nuc. Mat., 460 (2015) 221–225.
- [4] X. Wang, G. Li, Proc 180, Pu Futures 2014, Las Vegas
- [5] S. Vaudez, C. Marlot, J. Lechelle, J. Met. & Mat. Trans. E, 3, (2016) 107-111.
- [6] C. Guéneau, N. Dupin, Bo Sundman, C Martial, JC Dumas, S. Gosse, S. Chatain, F. De Bruycker, D. Manara, R. J. M.Konings, J. Nuc. Mat 419 (2011) 145-167.
- [7] Larché F., Cahn J.W. The interactions of composition and stress in crystalline solids. Acta Metall 33 (1985) 331–57.
- [8] Krishnamurthy R., Sheldon B.W. Stresses due to oxygen potential gradients in non-stoichiometric oxides. Acta Mater 52 (2004) 1807–1822.